Supporting Information

Van der Waals Stacked CdS /WSe_2 Heterostructure For High-Performance Photodetection

Lei Liu[a,b,d], Dafei Chen[a,b], Fan Mu[a,b], Yan Yang[a,b,d], Lujun Yang[a,b], Haiqiang Huang[a,b,d], Yifei Huang[a,b,d], Hui Zhang[a,b], Yingkai Liu[a,b,c,d,*]

[a] Institute of Physics and Electronic Information, Yunnan Normal University, Kunming 650500, China.

[b] Yunnan Key Laboratory of Opto-electronic Information Technology, Yunnan Normal University, Kunming 650500, China.

[c] Key Laboratory of Advanced Technique & Preparation for Renewable Energy Materials, Ministry of Education, Yunnan Normal University, Kunming 650500, China.

[d] Southwest United Graduate School, Kunming 650092, China.

[*] Correspondence: liuyingkai99@163.com;

Tel.: +86-871-6594-1166

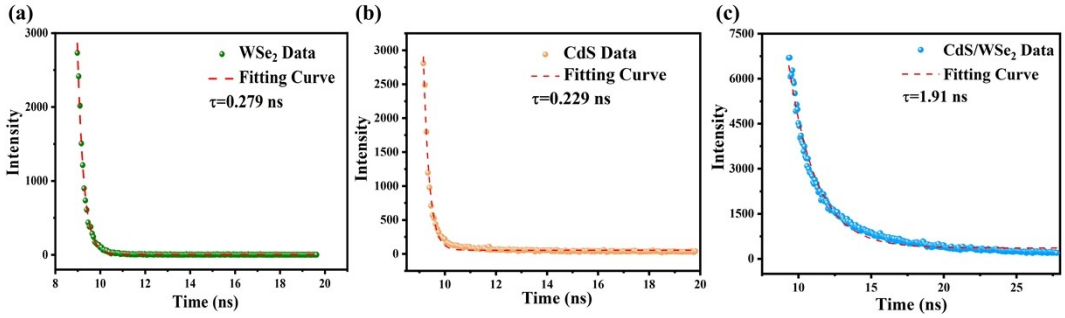

Figure S1. Time-resolved PL spectra of (a) isolated WSe_2 and (b) isolated CdS and CdS/WSe_2 HT.

Supporting Information

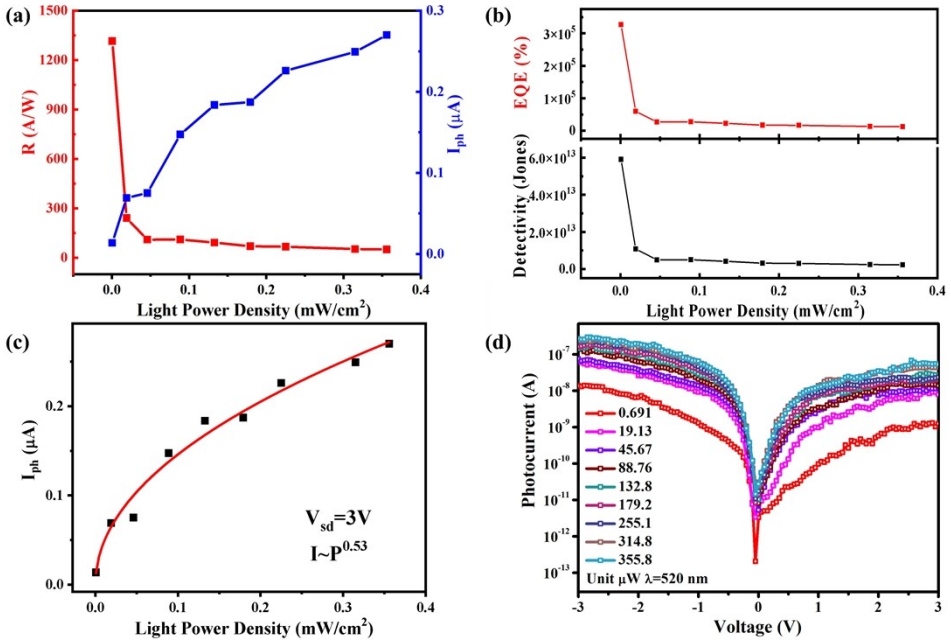

Figure S2. The incident light power of CdS/WSe_2 photodetector as a function of (a) photoresponse and photocurrent, (b) EQE and detectivity; (c)The relationship between photocurrent and incident light power density；(d) I-V curves (logarithmic form) at different optical powers. (the incident wavelength is 520 nm).

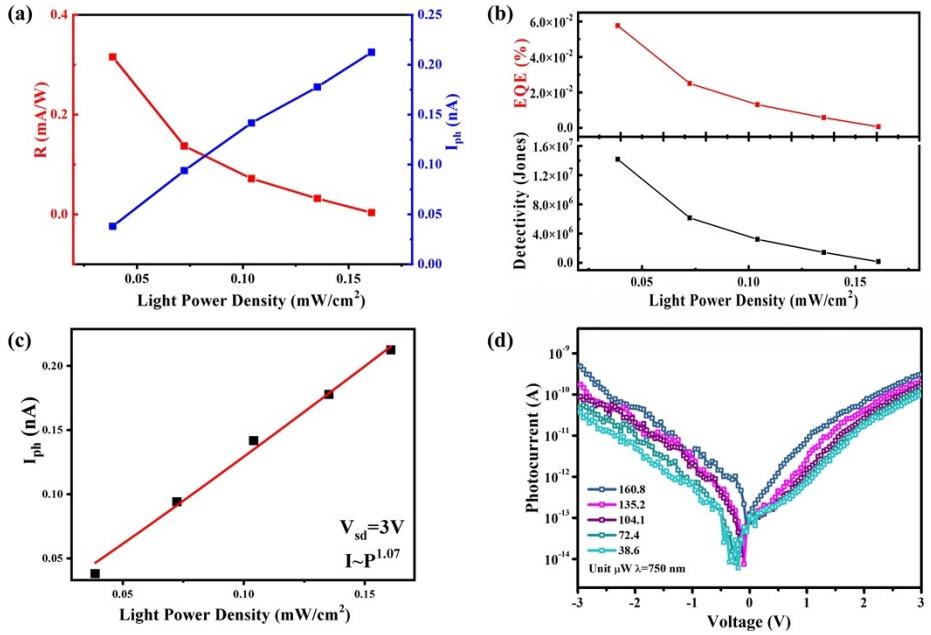

Figure S3. The incident light power of CdS/WSe_2 photodetector as a function of (a) photoresponse and photocurrent, (b) EQE and detectivity; (c)The relationship between photocurrent and incident light power density；(d) I-V curves (logarithmic form) at different optical powers. (the incident wavelength is 750 nm).

Supporting Information

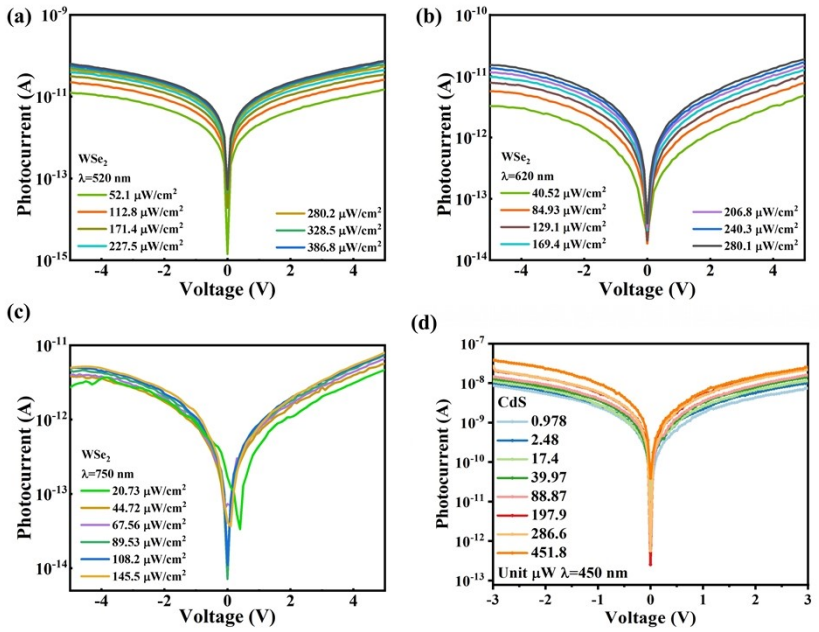

Figure S4. I-V curves (logarithmic form) of single WSe_2 at different optical powers. (the incident wavelength is 520 (a), 620 (b), 750 (c) nm, respectively); I-V curves (logarithmic form) of single CdS at different optical powers. (the incident wavelength is 450 (d) nm).

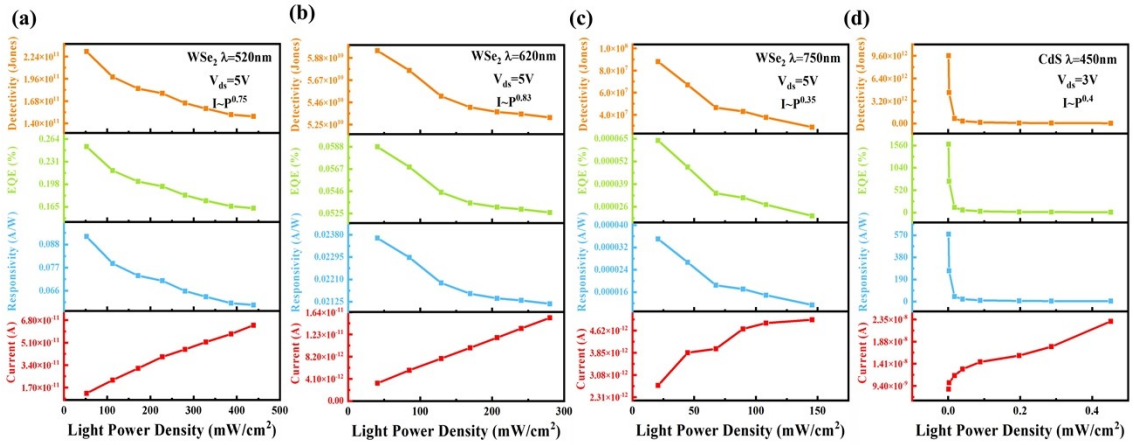

Figure S5. The photoelectric performance parameters of a single WSe_2 photodetector, with the incident light being 520 (a), 620 (b), and 750 (c) nm, respectively; The photoelectric performance parameters of a single CdS photodetector, with the incident light of 450 nm.

Supporting Information

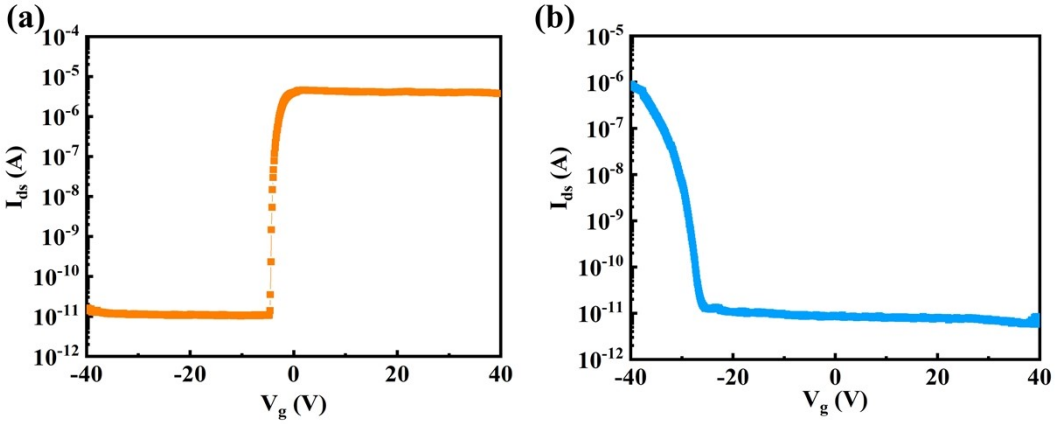

Figure S6. (a) Transfer characteristic curve of CdS-FET;
(b) Transfer characteristic curve of WSe_2-FET.

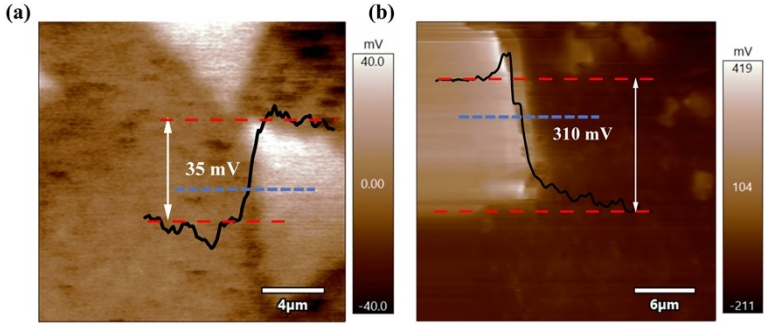

Figure S7. SKPFM characterization of the surface potential of (a) WSe_2/Au, (b) CdS/Au.

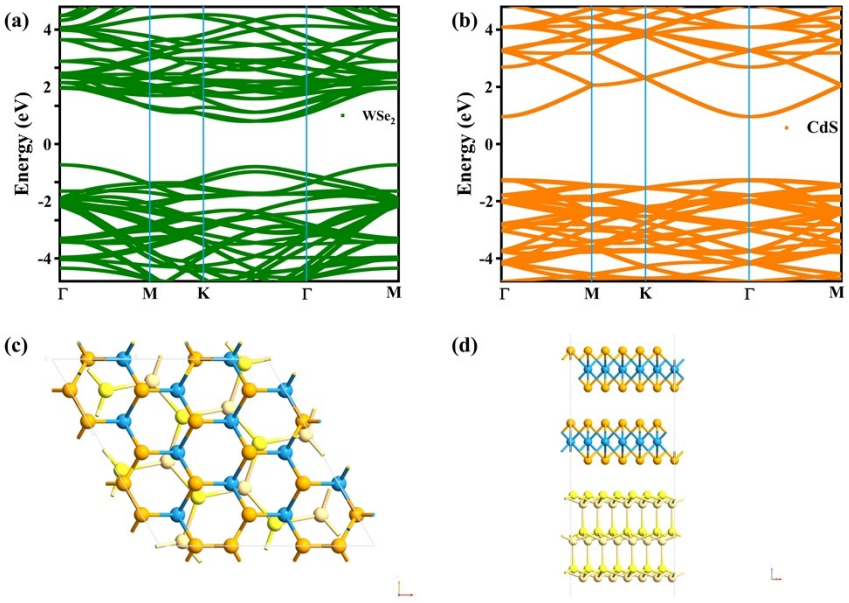

Figure S8. The calculated band structure for WSe_2 (a) and CdS (b) device along some high symmetry directions of the Brillouin zone; Top (c) and side (d) views of the heterojunction model used in the calculations.

Supporting Information

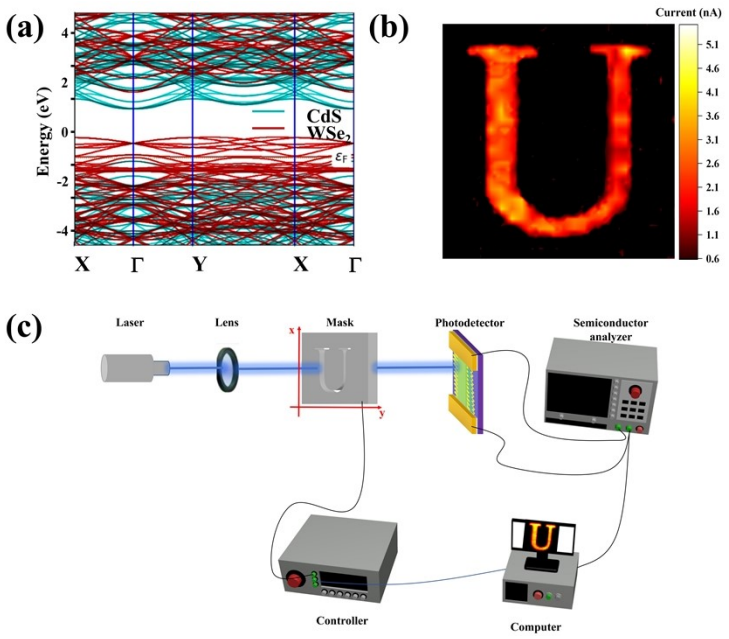

Figure S9. (a)The calculated band structure for CdS/WSe_2 HTs along some high symmetry directions of the Brillouin zone; (b) CdS/WSe_2 HTs photodetector imaging at 490 nm illumination (50 μW/cm^2, V_{ds} = 3V); (c) Schematic diagram of the imaging system.

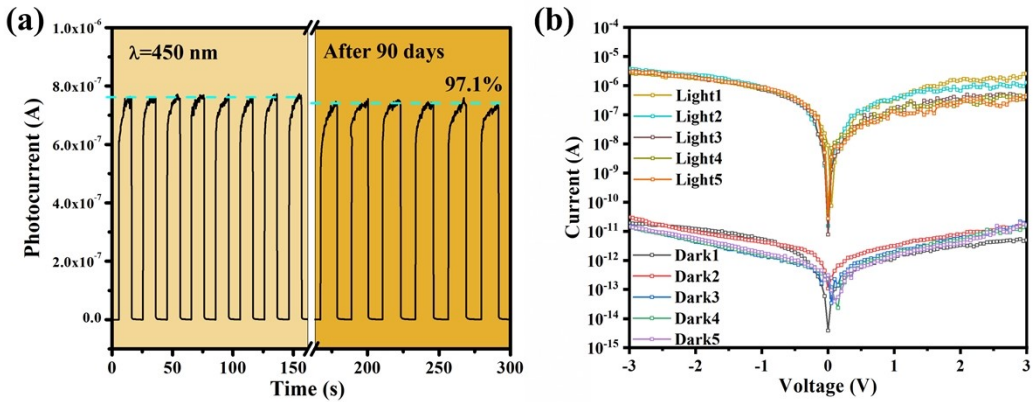

Figure S10. (a) The long-term stability tests of the WSe_2/CdS HTs under 450 nm (0.45 mW/cm^2) periodic illumination with 3 V bias voltage; (b) The reproducibility tests of five WSe_2/CdS HTs by 3 V under white-light illumination at controlled power densities (22.6 mW/cm^2) and dark condition.

Table S1 The reproducibility of WSe_2/CdS HTs devices

	I_{light} (-3V)	I_{light} (3V)	I_{dark} (-3V)	I_{dark} (3V)	On/off ratio (-3V)	On/off ratio (3V)
Mean	3.03×10^{-6}	1.02×10^{-6}	1.87×10^{-11}	1.42×10^{-11}	1.62×10^{5}	7.15×10^{4}
SD	4.87×10^{-7}	9.06×10^{-7}	6.95×10^{-12}	5.19×10^{-12}	3.63×10^{4}	5.10×10^{4}
RSD	16.06%	89.15%	37.12%	36.59%	22.46%	71.31%